BONE MODELING FOR CUSTOMIZED HYBRID BIOLOGICAL PROSTHESES DEVELOPMENT

Raffaella Aversa
Advanced Materials Lab, Department of Architecture and Industrial Design, Second University of Naples, Italy
E-mail: raffaella.aversa@unicampania.it

Relly Victoria V. Petrescu
0, Romania
E-mail: rvvpetrescu@gmail.com

Antonio Apicella
Advanced Materials Lab, Department of Architecture and Industrial Design, Second University of Naples, Italy
E-mail: antonio.apicella@unicampania.it

Florian Ion Tiberiu Petrescu
IFToMM, Romania
E-mail: fitpetrescu@gmail.com

ABSTRACT

Faithful modeling of the femur accounting for bone distribution and material orthotropic behavior is presented. In this study, a biofidel femur Finite Element Model (FEM) has been developed from Computerized Tomography (CT) scans using a specific combination of software's to correctly represent bone physiology and structural behavior. Proper identification of trabecular bone arrangement and distribution in the proximal diaphysis enabled modeling and definition of material properties. The faithful femur model proposed allows us to correctly account for non-isotropic properties to the proximal end explaining the critical structural role played by trabecular bone that should be taken into account in the design of a new innovative prosthetic system.

Keywords: Trabecular Bone, Biomimetic, Biomechanics, Prostheses.

1. INTRODUCTION

The human femur shows a high capacity to withstand external stresses and it is due to the mass distribution, morphology, and orthotropic behaviors of trabecular and cortical bone. Faithful modeling of the femur accounting for bone distribution and material orthotropic

107

behavior is presented. The use of biofidel model is aimed to develop an "in silico" tool that could enable the valuation of biomechanics modification induced by the alteration of the structural and morphological characteristics in prothesized bones.

Moreover, a faithful model assists us in the development of new design criteria for innovative prosthetic systems that, following the isostatic loading lines, could restore the physiological and natural stress and strains distribution. In this study, a biofidel femur Finite Element Model (FEM) has been developed from Computerized Tomography (CT) scans using a specific combination of software's to correctly represent bone physiology and structural behavior. Proper identification of trabecular bone arrangement and distribution in the proximal diaphysis enabled modeling and definition of material properties.

The faithful femur model proposed allows us to correctly account for non-isotropic properties to the proximal end explaining the critical structural role played by trabecular bone that should be taken into account in the design of a new innovative prosthetic system.

The human femur has been recognized to present a specific interior structure that is characterized by a high capacity to withstand external stresses while optimizing bone mass distribution and morphology to achieve this performance (Ashman *et al*., 1984; Dalstyra *et al*., 1993). This highly efficient structural behavior is due to the orthotropic behaviors of trabecular and cortical bone (Gottesman & Hashin, 1980; Oh & Harris, 1976).

The progressive physiological bone loss occurring at older age, which reduces bone toughness and capability to dissipate energy transmitted by a shock event, is the cause of aged people femur fracture. Internal structure of the femur proximal end defined by the Ward triangle is the anatomical region where the osteoporotic phenomenon alters the structural equilibrium increasing the possibility of femur neck fracture (Ashman & Rho, 1988; Burnstein *et al*., 1976; Carter & Hayes, 1977).

The necessity of predicting the structural modification induced by the alteration of the structural and morphological characteristic of the bone needs the development of faithful modeling of the femur accounting for bone distribution and material orthotropic behavior. This faithful model could enable us to design new prosthetic systems that restore the physiological and natural stress and strains distribution (Apicella *et al*., 2010: Gramanzini *et al*., 2016; Perillo *et al*., 2010, Rohlmann *et al*., 1982; Sorrentino *et al*., 2009; 2007).

A femur FEM model has been reconstructed here to correctly represent its structural behavior by modeling trabecular bone organization in the proximal end (femur head) and by defining for it material properties that are transversally isotropic. A comparison between femur model proposed and a model that allows isotropic properties to the proximal end makes evident that the first model explains structural role played by trabecular bone, defining, at the same way, a critical region in the femur neck (Abu-Lebdeh et al., 2019; Ashman et al., 1984; Dalstyra et al., 1993; Gottesman & Hashin, 1980; Oh & Harris, 1976; Ashman & Rho, 1988; Burnstein et al., 1976; Carter and Hayes, 1977; Apicella et al., 2002, 2010, 2018a-c: Duan et al., 2019; Gramanzini et al., 2016; Perillo et al., 2010; Rohlmann et al., 1982; Sorrentino et al., 2009, 2007; Aversa et al., 2019, 2018a-b, 2017 a-f, 2016 a-o, 2009; Crickmore, 1997; Donald, 2003; Goodall, 2003; Graham, 2002; Jenkins, 2001; Landis & Dennis, 2005; Petrescu & Petrescu, 2011-2012, 2013 a-c, 2014 a-c, 2015 a-c, 2016 a-b, 2017, 2019 a-d; Petrescu et al., 2018 a-o; 2017 a-u; Petrescu, 2019 a-n; Colvin, 2004; de Silva et al., 2006; Granato et al., 1994; Beaupre & Hayes, 1985; Reilly & Burstein, 1974; Reilly & Burnestain, 1975; Kaebernick et al., 2002; Mangun & Thurston, 2002; Murayama & Shu, 2001; Nazzaro, 1992; Kummer, 1986; Pliny & Elder, 1952; Tamburrino et al., 2018; Rogers-Hayden & Pidgeon, 2007).

2. MATERIALS AND METHODS

Medical Image Segmentation for Engineering application have been derived using the Mimics software (Materialise, Belgium) for processing patient medical image coming from CT. As reported in Figure 1, processing of CT resulted in a highly accurate 3D model of the patient pelvis anatomy.

This patient-specific model has been processed to develop new prosthetic engineering applications through a combined use of Mimics and 3-Matic (Materialise, Belgium) software's.

Namely, 3D solid and Finite Element Models (FEM) have been developed to simulate the external and internal morphology of the femur and other complex bone structures accounting for the orientation and densities of the head trabecular systems (Aversa *et al.*, 2009; Apicella *et al.*, 2010; Beaupre & Hayes, 1985; Reilly & Burstein, 1974; Reilly & Burnestain, 1975). The procedure is illustrated in the Figures from 2 to 5. The external geometry of femur has been reconstructed by generating a three-dimensional volume that interpolates the CT scans (Figure 2).
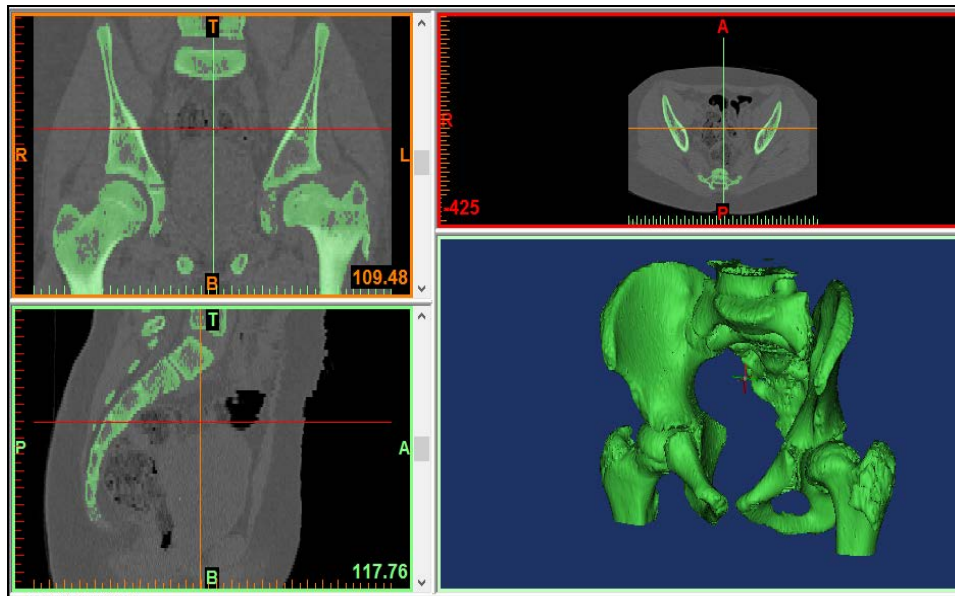
Figure 1: Biofidel medical Image from Computerized Tomography (CT) of a patient pelvis: Point clouds raw data

The results were then imported in the 3Matic software for surface and solid meshing optimization as indicated in Figure 3.

Internal modeling of the entire femur has been realized by defining three-dimensional internal tethraedric meshing distribution and size optimization (Figure 4).
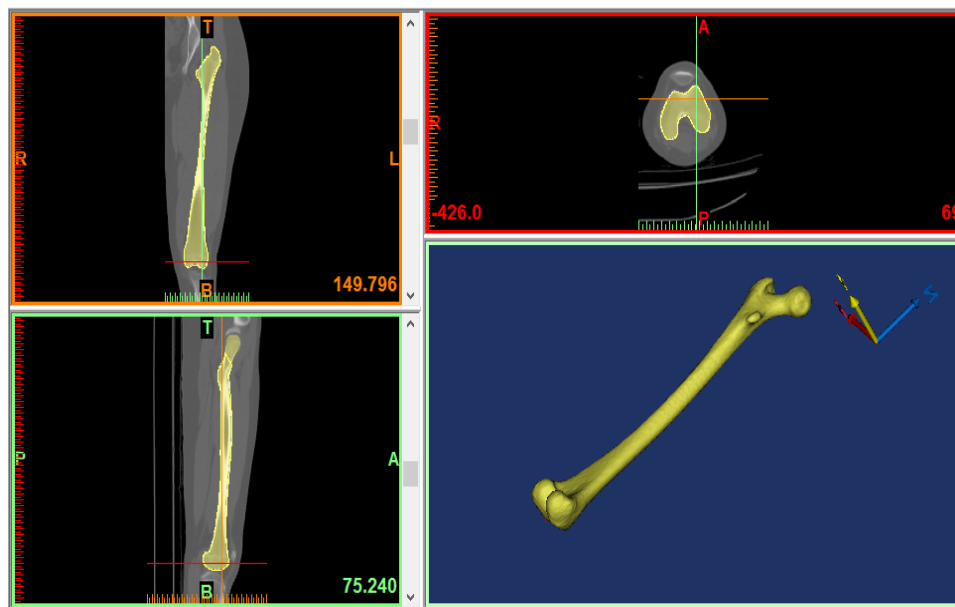

Figure 2: CT segmentations and Biofidel 3D solid modelling: Transverse (upper right), medial (upper left), frontal (lower left) and bone solid reconstruction of a patient femur (lower right)
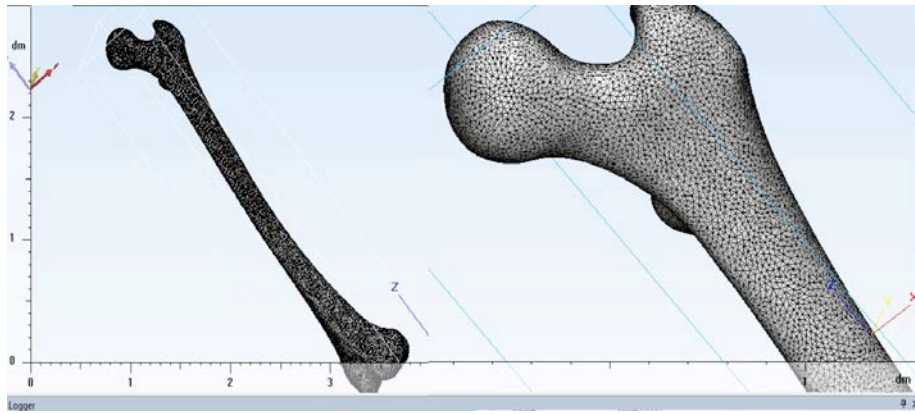
110

Figure 3: Preliminary triangle surface meshing optimization of the biofidel patient femur model
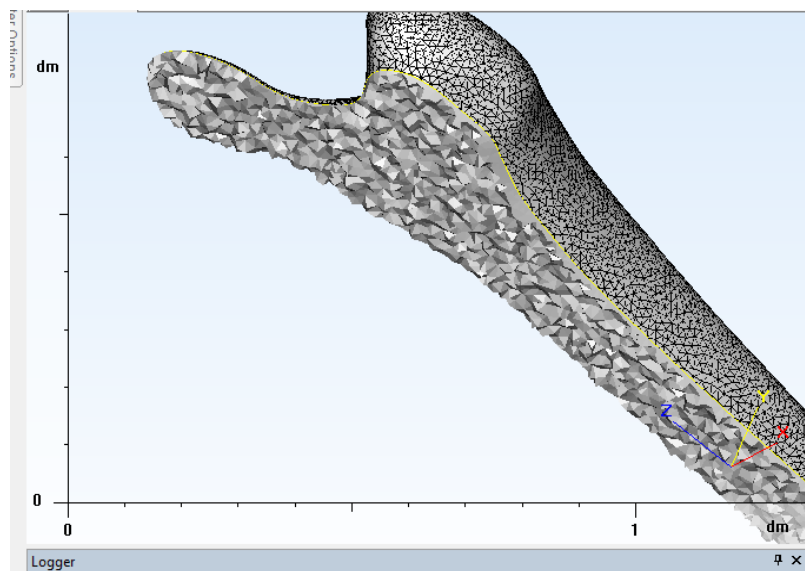

Figure 4: Tethraedric 3D solid meshing optimization of the biofidel patient femur model (detail of the proximal end)
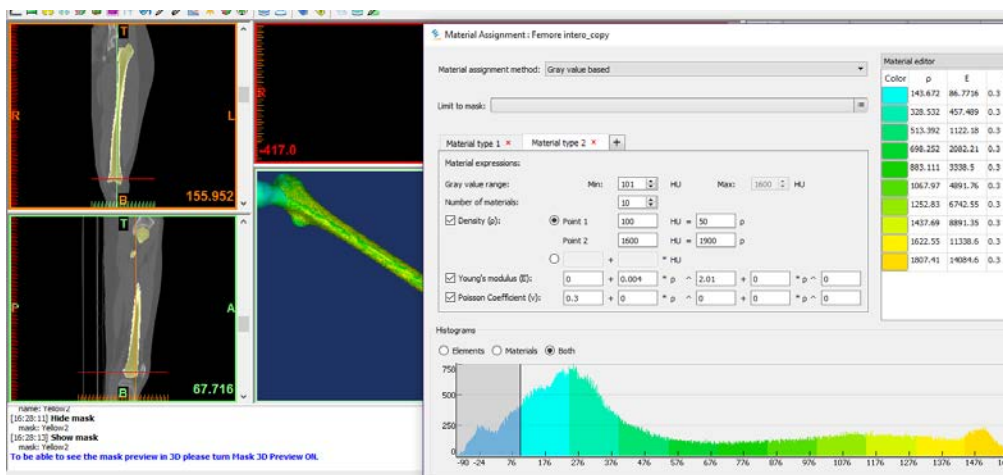

Figure 5: Material properties definition associated to the patient femur cortical and trabecular bone densities (left) and material properties assignation to HU bone densities (right)

The solid mesh elements have been successively associated to the bone densities measured according to the Hounsfield (HU) scale, which quantify the linear attenuation coefficients of X-rays in the tissues, and then assigned to the FEM model by the Mimics software (Figure 5).
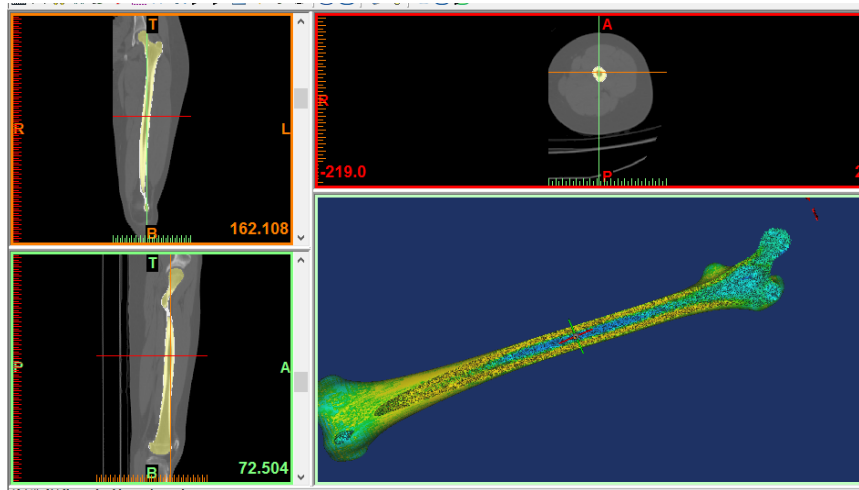

Figure 6: Material properties definition according to Hounsfield scale associated to the patient femur cortical and trabecular bone densities: Medial (upper left), Transverse (upper right) and Frontal (lower right) sections and 3D solid sectioned femur FEM

The evaluation of mechanical properties has been done considering the trabecular bone characteristics. The systems have been considered as transversally isotropic materials, with elastic and shear modulus expressed in terms of values of cortical bone and the values of elastic and shear modulus have been then evaluated multiplying those of cortical bone for the porosity defined for each tethraedric element by the Hounsfield (HU) densities scale. In this scale, the fat is worth about -110, the muscle about 40, the trabecular bone is in the range between 100 and 300 and the cortical bone extends beyond the trabecular bone values up to about 2000.

By operating on the internal structure and bone trabecular morphology, which represents the oriented trabecular system of proximal end, the solid mesh elements representing the trabecular-oriented material properties have been assigned (Figure 6) and the isotropic mechanical properties calculated as indicated in Table from the Figure 12.

At each tethraedric mesh element has been assigned by the software a color corresponding, according to the color property map reported in Table 1, to a specific mechanical isotropic mechanical property defined by the Hounsfield (HU) scale.

2.1.   Orthotropic Mechanical Properties Computation

The morphology of the porosity characterizing trabecular bone structure is related to the kind of state stress acting on the system. The different typology of trabecular bone porosity has made evident by the femur head internal structure (Figure 7).
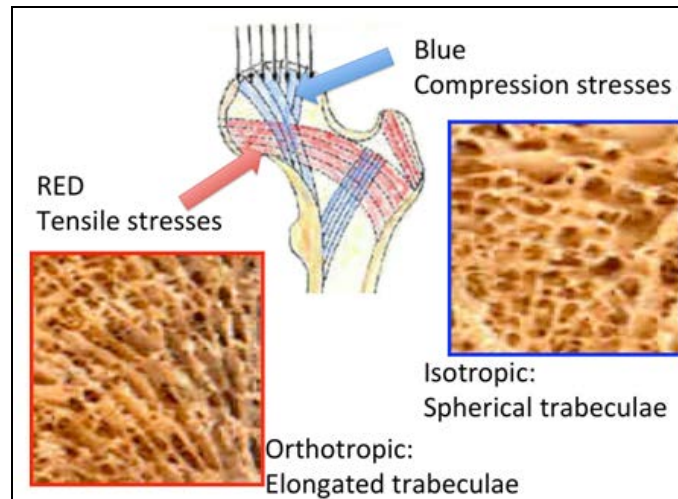

Figure 7: Stress state and morphology in the femur proximal epiphysis cortical and trabecular bone

The clear orientation of trabecular system observed in the lower left of Figure 6, which is observed in the area of the epiphysis subjected to tensile stresses, implicates that the tensile stress state is oriented in that direction; the absence of any directionality (namely a spherical morphology) indicates the absence of trabecular orientation that occurs in the volumes where the stress state is compressive. From the mechanical properties stand point of view, it can be inferred that the oriented trabecular volumes are characterized by orthotropic material properties while non-oriented ones show an isotropic material behavior.
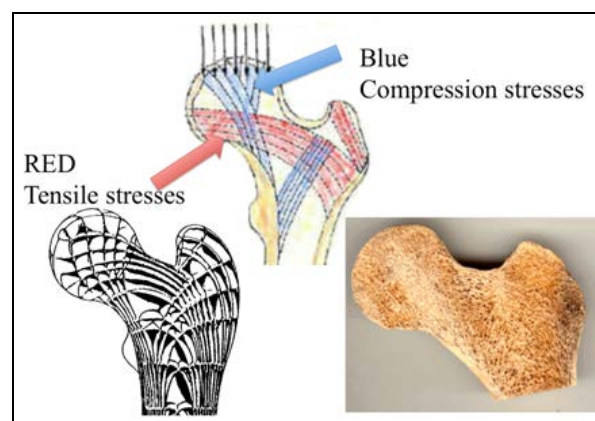

Figure 8: Kummer iso-tension lines (1986) mechanistic model and trabecular bone densities and orientations in a sectioned femur head

A mechanistic model of the hip proximal epiphysis has been proposed by Kummer (1986), which is related to the presence of isostatic lines characterizing the oriented trabecular systems, is reported in Figure 8. These morphological differences are better appreciated by comparing trabecular bone of oriented and non-oriented regions (Figure 7 and 8).

The previously CT computed values of bone densities have been then related to the isostatic lines of cortical and trabecular bone assigning to each tethraedric mesh element an orientation according to the stress isolines directions. This work defines a FEM model of human femur that could simulate geometrically the bone orthotropicity. The 3D solid and meshed FEM models have been exported in Solidworks software (Dassault Systèmes SolidWorks Corp.) to run the structural evaluations under specific biological loading conditions.

2.2.   FEM Analysis: Isotropic and Orthotropic Models

On the basis of 3D models two different material mechanical properties distribution have been developed and compared.

The first case considers the isotropic distribution of the mechanical properties over the entire femur while the second one assigns orthotropic mechanical properties to the proximal diaphysis (femur head).

2.2.1. Biometric Analysis

Before running the structural analysis it is necessary to define the personal characteristic biometric parameters of the patient femur-hip system. For this analysis was used the 3Matic software to:

- Identify the loading axis;

- Identify the center of the femoral head ball (creating a sphere that mediates the surface selected);

- Define the center of the joint epicondyle and mechanical axis of rotation of the knee.

The following parameters.

Once the biometric parameters have been identified, before the structural analysis it is necessary to define physiological loads and constrains.

2.2.2. Loads and Constrains

The force equilibrium condition in the monopodalic posture has been considered as a limiting loading condition.

This condition consists in the hip rotation equilibrium around the center of hip joint. It has been assumed that, in equilibrium, the sum of moment of body weight force and of gluteus muscular force is zero. It has been considered the patient body weight of 100 Kg, a gluteus muscular force applied to the great trochanter of 1800 N and a joint reaction force of 2740 N, which have been calculated from the equilibrium monopodalic equilibrium posture using the biometric parameters reported in Figure 9.

The equilibrium condition has been applied in the frontal plane, that is the plane defined by the mechanical axis and the hip joint center. Gluteus reaction force has been uniformly spread over 100 nodes of great trochanter region, while joint reaction force has been allocated on 50 nodes of the head (as indicated in the upper left of Figure 10).
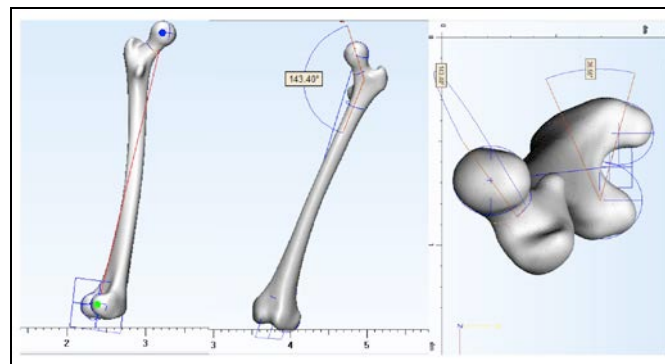

Figure 9: Biometric analysis: Mechanical axis of the femur, Angle of the femoral neck (143.40°), Divergence of the neck axis with the axis of epicondyles (36.65°)
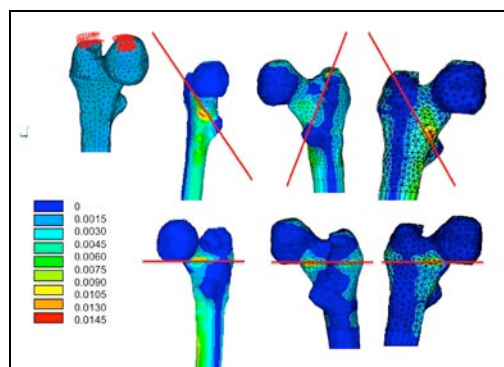

Figure 10: Equivalent Von Mises strains in the proximal diaphysis for orthotropic (upper) and isotropic (lower) trabecular bone properties. Red lines: Potential pertrochanteric femur fracture planes

115

3. RESULTS AND DISCUSSION;

The study is aimed to define a procedure to biofidelly model the femur structural behavior. Von Mises strain criterion has been used to compare and validate the two-trabecular properties mechanical properties distributions. This energetic criterion can quantify the capability of the bone to withstand high loads (Figure 10).

The orthotropic model realizes a more uniform strains distribution and better mimics the action of the load on the diaphysis.

The different structural behavior of the two models is also made evident by the Von Mises distribution of the strains, which are diverse at the back and frontal bone. Posteriorly, the strain distribution suggests the presence of flexure stress state, with maximum stress and strain distributed at the anatomical neck and great trochanter regions (upper part of Figure 10).

Furthermore, the orthotropic trabecular distribution is characterized by highest values of the strain distribution and energy at the femur of neck region; in this way, a more deformable region is detected in the anatomical region where the occurrence of pertrochanteric femur fractures are usually observed.
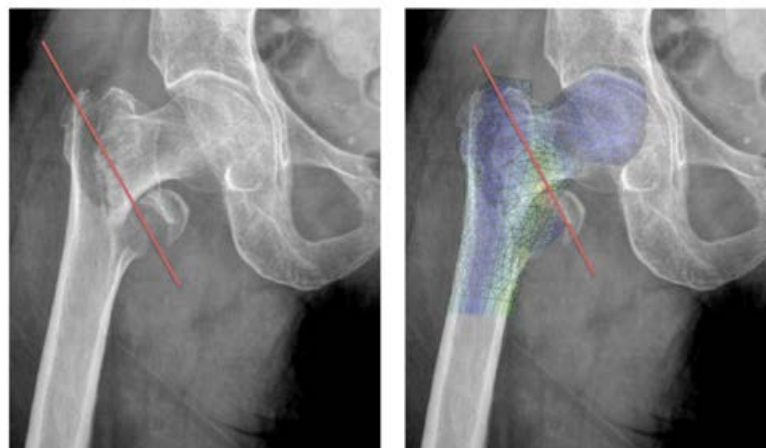

Figure 11: CT and fracture plane (red line) of a pertrochanteric femur fracture (left) compared to the fracture plane and strain distribution evaluated from the biofidel Finite Element Analysis for orthotropic distribution of the trabecular bone (right)

This area, named the Ward Triangle, is the region where the trabecular bone density reaches its minimum and where the bone loss in aged people is higher. For this reason, the probability to start a femur-neck fracture in this area is really high.

The Finite Element model adopting an orthotropic distribution of the trabecular mechanical properties is able to correctly predict the fracture behavior observed for these pertrochanteric femur fractures as can be inferred from the CT scan reported in the right part of Figure 11. In the right part of Figure 11, infact, the result of our analysis is overlying the actual CT image.

The fracture plane observed for a real fracture coincides with the plane fracture evaluated from the biofidel model developed in this study.

In the Figure 12 one can see a table with the isotropic mechanical properties assigned to the trabecular and cortical bone:

Material editor			
Color	ρ	E	v
	143.672	86.7716	0.3
	328.532	457.489	0.3
	513.392	1122.18	0.3
	698.252	2082.21	0.3
	883.111	3338.5	0.3
	1067.97	4891.76	0.3
	1252.83	6742.55	0.3
	1437.69	8891.35	0.3
	1622.55	11338.6	0.3
	1807.41	14084.6	0.3

Figure 12: Isotropic mechanical properties assigned to the trabecular and cortical bone

4. CONCLUSIONS

A biofidel femur Finite Element Model has been developed from CT scans using specific combination of software's to correctly represent bone physiology and structural behavior.

Proper identification of trabecular bone arrangement and distribution in the proximal diaphysis enabled modeling and definition of material properties. The faithful femur model proposed allows us to correctly account for non-isotropic properties to the proximal end explaining the critical structural role played by trabecular bone that should be taken into account in the design of new innovative prosthetic system.

The trabecular bone has been considered as a porous system, with a variable apparent density.

By comparing the mechanical behaviour of the spongeous bone, which can be seen as a trabecular bone without pores, the trabecular system, which has been modeled as differently

117

oriented parts, was characterized as an orthotropic materials while not oriented ones has been characterized as isotropic materials.

A comparison between a FEM analysis on this model and on the model that considers the proximal end as an isotropic material shows that the orthotropic model simulates a more realistic stress distribution in the bone because permits to simulate the structural role played by the trabecular systems, detecting clearly a bone crisis region.

A method to correctly approach the femur/neck fracture and the femur/prosthesis interface in a prosthesized bone have been than presented and it will be used in the design of new prosthetic systems.

REFERENCES

Abu-Lebdeh, T., Petrescu, R. V. V.; Al-Nasra, M., & Petrescu, F. I. T. (2019). Effect of nano-Silica (SiO2) on the Hydration Kinetics of Cement. **Engineering Review**, 39(3), 248-260. DOI: 10.30765/er.39.3.06.

Apicella, A. (2002) 'Innovative processes in production', in Anna Casotti and Editoriale Modo (Eds.): Designing the Future, the **Design of Matter**, Milano, Italy, 92–99.

Apicella, A., Aversa, R., & Petrescu, F. I. T. (2018a). Hybrid Ceramo-Polymeric Nano-Diamond Composites. **Am. J. Eng. Applied Sci.**, 11(2), 766-782. DOI: 10.3844/ajeassp.2018.766.782

Apicella, A., Aversa, R., & Petrescu, F. I. T. (2018b). Biomechanically Inspired Machines, Driven by Muscle Like Acting NiTi Alloys. **Am. J. Eng. Applied Sci.**, 11(2), 809-829. DOI: 10.3844/ajeassp.2018.809.829

Apicella, A., Aversa, R., Tamburrino, F., & Petrescu, F. I. T. (2018c). About the Internal Structure of a Bone and its Functional Role. **Am. J. Eng. Applied Sci.**, 11(2), 914-931. DOI: 10.3844/ajeassp.2018.914.931

Apicella, D., Aversa, R., Ferro, E., Ianniello, D., & Apicella, A. (2010). The importance of cortical bone orthotropicity, maximum stiffness direction and thickness on the reliability of mandible numerical models. **J. Biomed. Mater. Res. Part B Applied Biomater.**, 93, 150-163. DOI: 10.1002/jbm.b.31569

Ashman, R. B., Cowin, S. C., Van Buskirk, W. C., & Rice, J. C. (1984). A continuous wave technique for the measurement of the elastic properties of cortical bone. **J. Biomechan.**, 17, 349-361. DOI: 10.1016/0021-9290(84)90029-0

Ashman, R. B., & Rho, J. Y. (1988). Elastic modulus of trabecular bone material. **J. Biomechan.**, 21, 177-1781. DOI: 10.1016/0021-9290(88)90167-4

Aversa, R, Apicella, D., Perillo, L., Sorrentino, R., & Zarone, F.(2009). Non-linear elastic three-dimensional finite element analysis on the effect of endocrown material rigidity on alveolar bone remodeling process. **Dental Mater.**, 25, 678-690. DOI: 10.1016/j.dental.2008.10.015

Aversa, R., Petrescu, R. V. V., Apicella, A., & Petrescu, F. I. T. (2019). A Nanodiamond for Structural Biomimetic Scaffolds. **Engineering Review**, 39(1), 81-89. DOI: http://doi.org/10.30765/er.39.1.9

Aversa, R., Petrescu, R. V. V., Apicella, A., & Petrescu, F.I.T. (2017a). Nano-diamond hybrid materials for structural biomedical application. **Am. J. Biochem. Biotechnol.**, 13, 34-41. DOI: 10.3844/ajbbsp.2017.34.41

Aversa, R., Petrescu, R. V., Akash, B., Bucinell, R. B., & Corchado, J. M. (2017b). Kinematics and forces to a new model forging manipulator. **Am. J. Applied Sci.,** 14, 60-80. DOI: 10.3844/ajassp.2017.60.80

Aversa, R., Petrescu, R. V., Apicella, A., Petrescu, F. I. T., & Calautit, J. K. (2017c). Something about the V engines design. **Am. J. Applied Sci.**, 14, 34-52. DOI: 10.3844/ajassp.2017.34.52

Aversa, R., Parcesepe, D., Petrescu, R. V. V., & Chen, G. (2017d). Process ability of bulk metallic glasses. **Am. J. Applied Sci.**, 14, 294-301. DOI: 10.3844/ajassp.2017.294.301

Aversa, R., Petrescu, R. V. V., Akash, B., Bucinell, R. B., & Corchado, J. M. (2017e). Something about the balancing of thermal motors. **Am. J. Eng. Applied Sci.**, 10, 200.217. DOI: 10.3844/ajeassp.2017.200.217

Aversa, R., Petrescu, R. V. V., Apicella, A., Petrescu, F. I. T. (2017f). Modern Transportation and Photovoltaic Energy for Urban Ecotourism. **TRANSYLVANIAN REVIEW OF ADMINISTRATIVE SCIENCES** Special Issue, 5-20. DOI: 10.24193/tras.SI2017.1

Aversa, R., Petrescu, F. I. T., Petrescu, R. V., & Apicella, A. (2016a). Biomimetic FEA bone modeling for customized hybrid biological prostheses development. **Am. J. Applied Sci.**, 13, 1060-1067. DOI: 10.3844/ajassp.2016.1060.1067

Aversa, R., Parcesepe, D., Petrescu, R. V., Chen, G., & Petrescu, F. I. T. (2016b). Glassy amorphous metal injection molded induced morphological defects. **Am. J. Applied Sci.**, 13, 1476-1482. DOI: 10.3844/ajassp.2016.1476.1482

Aversa, R., Petrescu, R. V., Petrescu, F. I. T., & Apicella, A. (2016c). Smart-factory: Optimization and process control of composite centrifuged pipes. **Am. J. Applied Sci.**, 13, 1330-1341. DOI: 10.3844/ajassp.2016.1330.1341

Aversa, R., Tamburrino, F., Petrescu, R. V., Petrescu, F. I. T., & Artur, M. (2016d). Biomechanically inspired shape memory effect machines driven by muscle like acting NiTi alloys. **Am. J. Applied Sci.**, 13, 1264-1271. DOI: 10.3844/ajassp.2016.1264.1271

Aversa, R., Buzea, E. M., Petrescu, R. V., Apicella, A., & Neacsa, M. (2016e). Present a mechatronic system having able to determine the concentration of carotenoids. **Am. J. Eng. Applied Sci.**, 9, 1106-1111. DOI: 10.3844/ajeassp.2016.1106.1111

Aversa, R., Petrescu, R. V., Sorrentino, R., Petrescu, F. I. T., & Apicella, A. (2016f). Hybrid ceramo-polymeric nanocomposite for biomimetic scaffolds design and preparation. **Am. J. Eng. Applied Sci.**, 9, 1096-1105. DOI: 10.3844/ajeassp.2016.1096.1105

Aversa, R., Perrotta, V., Petrescu, R. V., Misiano, C., & Petrescu, F. I. T. (2016g). From structural colors to super-hydrophobicity and achromatic transparent protective coatings: Ion plating plasma assisted TiO_2 and SiO_2 nano-film deposition. **Am. J. Eng. Applied Sci.**, 9, 1037-1045. DOI: 10.3844/ajeassp.2016.1037.1045

119

Aversa, R., Petrescu, R. V., Petrescu, F. I. T. , & Apicella, A. (2016h). Biomimetic and evolutionary design driven innovation in sustainable products development. **Am. J. Eng. Applied Sci.,** 9, 1027-1036. DOI: 10.3844/ajeassp.2016.1027.1036

Aversa, R., Petrescu, R. V., Apicella, A., & Petrescu, F. I. T. (2016i). Mitochondria are naturally micro robots - a review. **Am. J. Eng. Applied Sci.**, 9, 991-1002. DOI: 10.3844/ajeassp.2016.991.1002

Aversa, R., Petrescu, R. V., Apicella, A., & Petrescu, F. I. T. (2016j). We are addicted to vitamins C and E-A review. **Am. J. Eng. Applied Sci.**, 9, 1003-1018. DOI: 10.3844/ajeassp.2016.1003.1018

Aversa, R., Petrescu, R. V., Apicella, A., & Petrescu, F. I. T. (2016k). Physiologic human fluids and swelling behavior of hydrophilic biocompatible hybrid ceramo-polymeric materials. **Am. J. Eng. Applied Sci.**, 9, 962-972. DOI: 10.3844/ajeassp.2016.962.972

Aversa, R., Petrescu, R. V., Apicella, A., & Petrescu, F. I. T. (2016l). One can slow down the aging through antioxidants. **Am. J. Eng. Applied Sci.**, 9, 1112-1126. DOI: 10.3844/ajeassp.2016.1112.1126

Aversa, R., Petrescu, R. V., Apicella, A., & Petrescu, F. I. T. (2016m). About homeopathy or ≪Similia Similibus Curentur≫. **Am. J. Eng. Applied Sci.**, 9, 1164-1172. DOI: 10.3844/ajeassp.2016.1164.1172

Aversa, R., Petrescu, R. V., Apicella, A., & Petrescu, F. I. T. (2016n). The basic elements of life's. **Am. J. Eng. Applied Sci.**, 9, 1189-1197. DOI: 10.3844/ajeassp.2016.1189.1197

Aversa, R., Petrescu, R. V., Apicella, A., & Petrescu, F. I. T. (2016o). Flexible stem trabecular prostheses. **Am. J. Eng. Applied Sci.**, 9, 1213-1221. DOI: 10.3844/ajeassp.2016.1213.122

Aversa, R., Apicella, A., Tamburrino, F., & Petrescu, F. I. T. (2018a). Mechanically Stimulated Osteoblast Cells Growth. **Am. J. Eng. Applied Sci.**, 11(2), 1023-1036. DOI: 10.3844/ajeassp.2018.1023.1036

Aversa, R., PARCESEPE, D., TAMBURRINO, F., Apicella, A., & Petrescu, F. I. T. (2018b). Cold Crystallization Behavior of a Zr44-Ti11-Cu10-Ni10-Be25 Metal Glassy Alloy. **Am. J. Eng. Applied Sci.**, 11(2), 1005-1022. DOI: 10.3844/ajeassp.2018.1005.1022

Beaupre, G. S., & Hayes, W. C., (1985). Finite element analysis of a three-dimensional open-celled model for trabecular bone. **J. Biomech. Eng.**, 107, 249-56. DOI: 10.1115/1.3138550

Burnstein, A., Reilly, D. T., & Martens, M. (1976). Aging of bone tissue: Mechanical properties. **J. Bone Joint Surgery**, 58, 82-86. PMID: 1249116

Carter, D. R., & Hayes, W. C. (1977). The compressive behavior of bone as a two-phase porous structure. **J. Bone Joint Surgery**, 59A, 954-962. PMID: 561786

Colvin, V. L. (2004). Sustainability for nanotechnology', **The Scientist**, 18(16), 26.

Crickmore, P. F. (1997). Lockheed's blackbirds-A-12, YF-12 and SR-71A. **Wings Fame**, 8, 30-93.

Dalstyra M., Huiskes, R., Odgaard, A., & Van Erning, L. (1993). Mechanical and textural properties of pelvic trabecular bone. **J. Biomechan.**, 26, 349-361. DOI: 10.1016/0021-9290(93)90014-6

De Silva, N., Jawahir, I. S., Dillon Jr., O. W., & Russell, M. (2006). A new comprehensive methodology for the evaluation of product sustainability at the design and development stage of consumer electronic products, **Int. J. Sustainable Manufacturing**, Vol. 1, No. 3, pp.251–264.

Donald, D. (2003). Lockheed's blackbirds: A-12, YF-12 and SR-71". **Black Jets**. AIRtime.

Duan, Y., Zhang, H., Sfarra, S., Avdelidis, N. P., Loutas, T. H., Sotiriadis, G., Kostopoulos, V., Fernandes, H., Petrescu, F. I., Ibarra-Castanedo, C., & Maldague, X. P. V. (2019). On the Use of Infrared Thermography and Acousto—Ultrasonics NDT Techniques for Ceramic-Coated Sandwich Structures. **Energies** 12(13), 1-12. DOI: 10.3390/en12132537

Gottesman, T., & Hashin, Z. (1980). Analysis of viscoelastic behaviour of bones on the basis of microstructure. **J. Biomechan.**, 13, 89-96. DOI: 10.1016/0021-9290(80)90182-7

Graham, R. H. (2002). SR-71 Blackbird: Stories, Tales and Legends. 1st Edn., **Zenith Imprint, North Branch, Minnesota**, ISBN-10: 1610607503.

Gramanzini, M., Gargiulo, S., Zarone, F., Megna, R., & Apicella A. (2016). Combined microcomputed tomography, biomechanical and histomorphometric analysis of the peri-implant bone: A pilot study in minipig model. **Dental Mater.**, 32, 794-806. DOI: 10.1016/j.dental.2016.03.025

Granato, A., Apicella, A., & Montanino, M. (1994). Utilization of fluorinated polymers in surface protection of zeolite bearing tuff, **Materials Engineering**,. 5, 329–342.

Goodall, J. (2003). Lockheed's SR-71 "Blackbird" Family. Hinckley, UK: **Aerofax/Midland Publishing**, 2003. (ISBN 1-85780-138-5).

Jenkins, D. R., (2001). Lockheed Secret Projects: Inside the Skunk Works. 1st Edn., **Zenith Imprint, St. Paul, Minnesota: MBI Publishing Company**, ISBN-10: 1610607287.

Kaebernick, H., Anityasari, M., & Kara, S. (2002). A technical and economic model for end-of-life (EOL) options of industrial products, **International Journal of Environmental and Sustainable Development**, 1, 171–183.

Kummer, B. (1986). Biomechanical principles of the statistics of the hip joint. A critical appraisal of a new theory, **Zeitschrift fur Orthopadie und Ihre Grenzgebiete**, 124, 179-187. DOI: 10.1055/s-2008-1044544

Landis, T. R., & Dennis, R. J. (2005). Lockheed Blackbirds. 1st Edn., **Specialty Press, North Branch**, ISBN-10: 1580070868, pp: 104.

Mangun, D., & Thurston, D. L. (2002). Incorporating component reuse, remanufacture and recycle into product portfolio design, **IEEE Transactions on Engineering Management**, 49, 479–490.

Murayama, T., & Shu, L. H. (2001). Treatment of reliability for reuse and remanufacture, **Proceedings of EcoDesign 2001**: The 2nd International Symposium on Environmentally Conscious Design and Inverse Manufacturing, Tokyo, Japan, pp.287–292.

Nazzaro W. W. (1992). Radon transport from soil to air, **Review of Geophysics**, Vol. 30, pp.137–160.

Oh, I., & Harris, W. H. (1976). Proximal strain distribution in the loaded femur. An in vitro comparison of the distributions in the intact femur and after insertion of different hip-replacement femoral components. **J. Bone Joint Surgery**, 60, 75-85. PMID: 624762

Perillo, L., Sorrentino, R., Apicella, D., Quaranta, A., & Gherlone, C. (2010). Nonlinear visco-elastic finite element analysis of porcelain veneers: A submodelling approach to strain and stress distributions in adhesive and resin cement. **J. Adhesive Dent**., 12, 403-413.

Petrescu, F. I., & Petrescu, R. V. (2012). New Aircraft II. 1st Edn., **Books On Demand**, 138.

Petrescu, F. I., & Petrescu, R. V. (2011). Memories about flight. 1st Edn., **CreateSpace**, 652.

Petrescu, F. I. T., & Petrescu, R. (2014a). Parallel moving mechanical systems. **Independent J. Manage. Product.**, 5, 564-580.

Petrescu, F. I. T., & Petrescu, R. (2014b). Cam gears dynamics in the classic distribution. **Independent J. Manage. Product.**, 5, 166-185.

Petrescu, F. I. T., & Petrescu, R. (2014c). High-efficiency gears synthesis by avoid the interferences. **Independent J. Manage. Product.**, 5, 275-298.

Petrescu, F. I. T., & Petrescu, R. (2015a). Forces at the main mechanism of a railbound forging manipulator. **Independent J. Manage. Product.**, 6, 904-921.

Petrescu, F. I. T., & Petrescu, R. (2015b). Kinematics at the main mechanism of a railbound forging manipulator. **Independent J. Manage. Product.**, 6, 711-729.

Petrescu, F. I. T., & Petrescu, R. (2015c). Machine motion equations. **Independent J. Manage. Product.**, 6, 773-802.

Petrescu, F. I. T., & Petrescu, R. (2016a). Dynamic cinematic to a structure 2R. **Revista Geintec-Gestao Inovacao E Tecnol.**, 6, 3143-3154.

Petrescu, F. I. T., & Petrescu, R. (2016b). An Otto engine dynamic model. **Independent J. Manage. Product.**, 7, 038-048.

Petrescu, F. I. T., & Petrescu, R. V. V. (2019a). Nuclear hydrogen structure and dimensions, **International Journal of Hydrogen Energy**, 44(21):10833-10837. https://doi.org/10.1016/j.ijhydene.2019.02.140

Petrescu, F. I. T. (2018a). Inverse Kinematics to a Stewart Platform. **J M E S** 5(2),111-122.

Petrescu, F. I. T. (2017b). The Computer Algorithm for Machine Equations of Classical Distribution. **J M E S** 4(4), 193-209.

Petrescu, F. I. T. (2019). About the nuclear particles' structure and dimensions. **Comp. Part. Mech.** 6(2), 191-194. https://doi.org/10.1007/s40571-018-0206-7

Petrescu, N., & Petrescu, F. I. T. (2019b). The Yield of the Thermal Engines. **Journal of Mechatronics and Robotics** 3, 215-236. DOI: 10.3844/jmrsp.2019.215.236

Petrescu, N., & Petrescu, F. I. T. (2019c). Machine Motion Equations Presented in a New General Format. **Journal of Mechatronics and Robotics** 3, 344-377. DOI: 10.3844/jmrsp.2019.344.377

Petrescu, N., & Petrescu, F. I. T. (2019d). New About the Balancing of Thermal Motors. **Journal of Mechatronics and Robotics** 3, 471-496. DOI: 10.3844/jmrsp.2019.471.496

Petrescu, N., Aversa, R., Apicella, A., & Petrescu, F. I. T. (2018n). Something about Robots Today. **Journal of Mechatronics and Robotics** 2, 85-104. DOI: 10.3844/jmrsp.2018.85.104

Petrescu, N., Aversa, R., Apicella, A., & Petrescu, R. V. (2018o). Structural-Topological Synthesis of Planar Mechanisms with Rods and Wheels. **Journal of Mechatronics and Robotics** 2:105-120. DOI: 10.3844/jmrsp.2018.105.120

Petrescu, R. V., & Petrescu, F. I. (2013a). Lockheed Martin. 1st Edn., **CreateSpace**, 114.

Petrescu, R. V., & Petrescu, F. I. (2013b). Northrop. 1st Edn., **CreateSpace**, 96.

Petrescu, R. V., & Petrescu, F. I. (2013c). The aviation history or new aircraft I color. 1st Edn., **CreateSpace**, 292.

Petrescu, R. V. (2017a). Energia verde para proteger o meio ambiente, **Geintec**, 7(1),3722-3743.

Petrescu, R. V., Aversa, R., Apicella, A., & Petrescu, F. I. T. (2018j). Romanian engineering "on the wings of the wind". **J. Aircraft Spacecraft Technol.**, 2, 1-18. DOI: 10.3844/jastsp.2018.1.18

Petrescu, R. V., Aversa, R., Apicella, A. & Petrescu, F. I. T. (2018b). NASA Data used to discover eighth planet circling distant star. **J. Aircraft Spacecraft Technol.**, 2, 19-30. DOI: 10.3844/jastsp.2018.19.30

Petrescu, R. V., Aversa, R., Apicella, A. & Petrescu, F. I. T. (2018c). NASA has found the most distant black hole. **J. Aircraft Spacecraft Technol.**, 2, 31-39. DOI: 10.3844/jastsp.2018.31.39

Petrescu, R. V., Aversa, R., Apicella, A. & Petrescu, F. I. T. (2018d). Nasa selects concepts for a new mission to titan, the moon of saturn. **J. Aircraft Spacecraft Technol.**, 2, 40-52. DOI: 10.3844/jastsp.2018.40.52

Petrescu, R. V., Aversa, R., Apicella, A. & Petrescu, F. I. T. (2018e). NASA sees first in 2018 the direct proof of ozone hole recovery. **J. Aircraft Spacecraft Technol.**, 2, 53-64. DOI: 10.3844/jastsp.2018.53.64

Petrescu, R. V., Aversa, R., Akash, B., Bucinell, R., & Corchado, J. (2017c). Modern propulsions for aerospace-a review. **J. Aircraft Spacecraft Technol.,** 1, 1-8. DOI: 10.3844/jastsp.2017.1.8

Petrescu, R. V., Aversa, R., Akash, B., Bucinell, R., & Corchado, J. (2017d). Modern propulsions for aerospace-part II. **J. Aircraft Spacecraft Technol.**, 1, 9-17. DOI: 10.3844/jastsp.2017.9.17

Petrescu, R. V., Aversa, R., Akash, B., Bucinell, R., & Corchado, J. (2017e). History of aviation-a short review. **J. Aircraft Spacecraft Technol.**, 1, 30-49. DOI: 10.3844/jastsp.2017.30.49

Petrescu, R. V., Aversa, R., Akash, B., Bucinell, R., & Corchado, J. (Bucinell, R., & Corchado, J. (2017f). Lockheed martin-a short review. **J. Aircraft Spacecraft Technol.**, 1, 50-68. DOI: 10.3844/jastsp.2017.50.68

Petrescu, R. V., Aversa, R., Akash, B., Bucinell, R., & Corchado, J. (J. CORCHADO *et al.*, 2017g. Our universe. **J. Aircraft Spacecraft Technol.**, 1: 69-79. DOI: 10.3844/jastsp.2017.69.79

Petrescu, R. V., Aversa, R., Akash, B., & Corchado, J. (2017h). What is a UFO? **J. Aircraft Spacecraft Technol.**, 1: 80-90. DOI: 10.3844/jastsp.2017.80.90

Petrescu, R. V., Aversa, R., Akash, B., & Corchado, J. (2017i). About bell helicopter FCX-001 concept aircraft-a short review. **J. Aircraft Spacecraft Technol.**, 1, 91-96. DOI: 10.3844/jastsp.2017.91.96

Petrescu, R. V., Aversa, R., Akash, B., & Corchado, J. (2017j). Home at airbus. **J. Aircraft Spacecraft Technol.**, 1, 97-118. DOI: 10.3844/jastsp.2017.97.118

Petrescu, R. V., Aversa, R., Akash, B., & Corchado, J. (2017k). Airlander. **J. Aircraft Spacecraft Technol.**, 1, 119-148. DOI: 10.3844/jastsp.2017.119.148

Petrescu, R. V., Aversa, R., Akash, B., & Corchado, J. (2017l). When boeing is dreaming-a review. **J. Aircraft Spacecraft Technol.**, 1, 149-161. DOI: 10.3844/jastsp.2017.149.161

Petrescu, R. V., Aversa, R., Akash, B., & Corchado, J. (2017m). About Northrop Grumman. **J. Aircraft Spacecraft Technol.**, 1, 162-185. DOI: 10.3844/jastsp.2017.162.185

Petrescu, R. V., Aversa, R., Akash, B., & Corchado, J. (2017n). Some special aircraft. **J. Aircraft Spacecraft Technol.**, 1, 186-203. DOI: 10.3844/jastsp.2017.186.203

Petrescu, R. V., Aversa, R., Akash, B., & Corchado, J. (2017o). About helicopters. **J. Aircraft Spacecraft Technol.**, 1, 204-223. DOI: 10.3844/jastsp.2017.204.223

Petrescu, R. V., Aversa, R., Akash, B., & Apicella, A. (2017p). The modern flight. **J. Aircraft Spacecraft Technol.**, 1, 224-233. DOI: 10.3844/jastsp.2017.224.233

Petrescu, R. V., Aversa, R., Akash, B., & Apicella, A. (2017q). Sustainable energy for aerospace vessels. **J. Aircraft Spacecraft Technol.**, 1, 234-240. DOI: 10.3844/jastsp.2017.234.240

Petrescu, R. V., Aversa, R., Akash, B., & Apicella, A. (2017r). Unmanned helicopters. **J. Aircraft Spacecraft Technol.**, 1, 241-248. DOI: 10.3844/jastsp.2017.241.248

Petrescu, R. V., Aversa, R., Akash, B., & Apicella, A. (2017s). Project HARP. **J. Aircraft Spacecraft Technol.**, 1, 249-257. DOI: 10.3844/jastsp.2017.249.257

Petrescu, R. V., Aversa, R., Akash, B., & Apicella, A. (2017t). Presentation of Romanian engineers who contributed to the development of global aeronautics-part I. **J. Aircraft Spacecraft Technol.**, 1, 258-271. DOI: 10.3844/jastsp.2017.258.271

Petrescu, R. V., Aversa, R., Akash, B., & Apicella, A. (2017u). A first-class ticket to the planet mars, please. **J. Aircraft Spacecraft Technol.**, 1, 272-281. DOI: 10.3844/jastsp.2017.272.281

Petrescu, R. V., Aversa, R., Apicella, A., & Kozaitis, S. (2018f). NASA started a propeller set on board voyager 1 after 37 years of break. **Am. J. Eng. Applied Sci.**, 11, 66-77. DOI: 10.3844/ajeassp.2018.66.77

Petrescu, R. V., Aversa, R., Apicella, A., & Kozaitis, S. (2018g). There is life on mars? **Am. J. Eng. Applied Sci.**, 11, 78-91. DOI: 10.3844/ajeassp.2018.78.91

Petrescu, R. V., Aversa, R., Abu-Lebdeh, T. M., Apicella, A., & Petrescu, F. I. T. (2018h). NASA satellites help us to quickly detect forest fires. **Am. J. Eng. Applied Sci.**, 11, 288-296. DOI: 10.3844/ajeassp.2018.288.296

Petrescu, R. V., Aversa, R., Apicella, A., & Petrescu, F. I. T. (2018i). Total Static Balancing and Kinetostatics of the 3R Base Cinematic Chain. **Journal of Mechatronics and Robotics** 2, 1-13. DOI: 10.3844/jmrsp.2018.1.13

Petrescu, R. V., Aversa, R., Apicella, A., & Petrescu, F. I. T. (2018j). Switching from Flat to Spatial Motion to 3R Mechatronic Systems. **Journal of Mechatronics and Robotics** 2, 14-22. DOI: 10.3844/jmrsp.2018.14.22

Petrescu, R. V., Aversa, R., Apicella, A., & Petrescu, F. I. T. (2018k). The Dynamics of the Planar Cinematic Balanced Chain at the Plan Module 3R. **Journal of Mechatronics and Robotics** 2, 23-34. DOI: 10.3844/jmrsp.2018.23.34

Petrescu, R. V., Aversa, R., Apicella, A., & Petrescu, F. I. T. (2018l). Dynamic Kinematics of the Plan Balanced Chain at the Planar Module 3R. **Journal of Mechatronics and Robotics** 2, 35-44. DOI: 10.3844/jmrsp.2018.35.44

Petrescu, R. V., Aversa, R., Apicella, A., & Petrescu, F. I. T. (2018m). Inverse Kinematics of a Stewart Platform. **Journal of Mechatronics and Robotics** 2, 45-59. DOI: 10.3844/jmrsp.2018.45.59

Petrescu, R. V. V. (2019b). About the Space Robots. **Journal of Mechatronics and Robotics** 3:1-32. DOI: 10.3844/jmrsp.2019.1.32

Petrescu, R. V. V. (2019c). Medical Service of Robots. **Journal of Mechatronics and Robotics** 3, 60-81. DOI: 10.3844/jmrsp.2019.60.81

Petrescu, R. V. V. (2019d). Dynamics at Classical Distribution. **Journal of Mechatronics and Robotics** 3,82-101. DOI: 10.3844/jmrsp.2019.82.101

Petrescu, R. V. V. (2019e). Time Factory. **Journal of Mechatronics and Robotics** 3, 102-121. DOI: 10.3844/jmrsp.2019.102.121

Petrescu, R. V. V. (2019f). About Robotics, Mechatronics and Automation that Help us Conquer the Cosmic Space. **Journal of Mechatronics and Robotics** 3, 129-155. DOI: 10.3844/jmrsp.2019.129.155

Petrescu, R. V. V. (2019g). Dynamic Models for Rigid Memory Mechanisms. **Journal of Mechatronics and Robotics** 3, 156-183. DOI: 10.3844/jmrsp.2019.156.183

Petrescu, R. V. V. (2019h). Something about a Railbound Forging Manipulator. **Journal of Mechatronics and Robotics** 3, 184-207. DOI: 10.3844/jmrsp.2019.184.207

Petrescu, R. V. V. (2019i). Face Recognition as a Biometric Application. **Journal of Mechatronics and Robotics** 3, 237-257. DOI: 10.3844/jmrsp.2019.237.257

Petrescu, R. V. V. (2019j). Contributions to the Synthesis of Fixed Axle Gears by Avoiding the Interference Phenomenon. **Journal of Mechatronics and Robotics** 3, 280-300. DOI: 10.3844/jmrsp.2019.280.300

Petrescu, R. V. V. (2019k). Space Probes. **Journal of Mechatronics and Robotics** 3, 301-343. DOI: 10.3844/jmrsp.2019.301.343

Petrescu, R. V. V. (2019l). Presents Some Aspects and Applications of Projective Geometry. **Journal of Mechatronics and Robotics** 3, 389-430. DOI: 10.3844/jmrsp.2019.389.430

Petrescu, R. V. V. (2019m). Mechanisms With Rigid Memory. **Journal of Mechatronics and Robotics** 3, 431-470. DOI: 10.3844/jmrsp.2019.431.470

Petrescu, R. V. V. (2019n). Internal Combustion Engines Forces. **Journal of Mechatronics and Robotics** 3, 497-520. DOI: 10.3844/jmrsp.2019.497.520

PLINY the ELDER (AD 77) (1952) Naturalis Historia, **reprint de Loeb Classical Lib. Univ. Press**, E.H. Warmington Ed. Cambridge.

REILLY, D. T., & BURNESTAIN, A. H. (1975). The elastic and ultimate properties of compact bone tissue. **J. Biomechan.**, 8, 393-405. DOI: 10.1016/0021-9290(75)90075-5

125

Reilly, D. T., & Burnestain, A. H. (1974). The mechanical properties of cortical bone. **J. Bone Joint Surgery**, 56, 1001-1021. http://jbjs.org/content/56/5/1001.short

Rogers-Hayden, T., & Pidgeon, N. (2007). Development in nanotechnology public engagement in the UK: upstream toward sustainability?, **Journal of Cleaner Production**, 6, 8–9.

Rohlmann, A., Mossner, U., Bergmann, G., & Kolbel, R. (1982). Finite-element-analysis and experimental investigation of stresses in a femur. **J. Biomed. Eng.**, 4, 241-246. DOI: 10.1016/0141-5425(82)90009-7

Sorrentino, R., Aversa, R., Ferro, V., Auriemma, T., & Zarone, F. (2007). Three-dimensional finite element analysis of strain and stress distributions in endodontically treated maxillary central incisors restored with diferent post, core and crown materials. **Dent Mater.**, 23, 983-993. DOI: 10.1016/j.dental.2006.08.006

Sorrentino, R., Apicella, D., Riccio, C., Gherlone, E. D., & Zarone, F. (2009). Nonlinear visco-elastic finite element analysis of different porcelain veneers configuration. **J. Biomed. Mater. Res. Part B Applied Biomater.**, 91, 727-736. DOI: 10.1002/jbm.b.31449

Tamburrino, F., Apicella, A., Aversa, R., & Petrescu, F. I. T. (2018). Advanced Manufacturing for Novel Materials in Industrial Design Applications. **Am. J. Eng. Applied Sci.**, 11(2), 932-972. DOI: 10.3844/ajeassp.2018.932.972